Quantum transport of bosonic cold atoms in double-well optical lattices

Yinyin Qian, Ming Gong, and Chuanwei Zhang*
Department of Physics and Astronomy, Washington State University, Pullman, Washington 99164, USA
(Received 21 February 2011; published 18 July 2011)

We numerically investigate, using the time evolving block decimation algorithm, the quantum transport of ultracold bosonic atoms in a double-well optical lattice through slow and periodic modulation of the lattice parameters (intra- and inter-well tunneling, chemical potential, etc.). The transport of atoms does not depend on the rate of change of the parameters (as along as the change is slow) and can distribute atoms in optical lattices at the quantized level without involving external forces. The transport of atoms depends on the atom filling in each double well and the interaction between atoms. In the strongly interacting region, the bosonic atoms share the same transport properties as noninteracting fermions with quantized transport at the half filling and no atom transport at the integer filling. In the weakly interacting region, the number of the transported atoms is proportional to the atom filling. We show the signature of the quantum transport from the momentum distribution of atoms that can be measured in the time-of-flight image. A semiclassical transport model is developed to explain the numerically observed transport of bosonic atoms in the noninteracting and strongly interacting limits. The scheme may serve as an quantized battery for atomtronics applications.

DOI: 10.1103/PhysRevA.84.013608 PACS number(s): 03.75.Lm, 03.65.Vf

I. INTRODUCTION

Quantum charge pumping, a coherent quantum transport process that generates steady charge currents of electrons through adiabatically and periodically time-varying potentials, is a standard method for charge transport in solid-state circuits [1–5]. In quantized charge transport, the number of particles pumped out during each cycle of the potential modulation is an integer and can be understood using a Berry phase [6]. Because of the precise control on the amount of pumped charges at the single-electron level, quantum charge pumping has found important applications in many electronic devices [7,8]. It also provides a solid foundation to the modern theory of electric polarization [9–11]. Similar ideas have also been extended to another degree of freedom of electrons, the spin, leading to the quantum spin pumping that plays a crucial role in spintronics [12–14]. However, the exact quantized charge transport is usually difficult to observe in experiments because of unavoidable complexity due to impurities, disorder, and interactions in the solid.

In view of the significance of electronics and spintronics, there has been a great deal of interest recently in developing a one-to-one analog of complex and interesting electronic materials, circuits, and devices using ultracold neutral atoms [15–17]. This field, known as atomtronics, is a significant extension of the recent great efforts on emulating condensed matter physics using ultracold atoms [18–20]. Important concepts such as atomic batteries, diodes, and transistors have been proposed recently for atomtronics. It would be natural and also important to investigate the coherent quantum transport process of cold atoms in optical lattices, which is an important element of atomtronic devices. A straightforward method for the transport, of course, is by applying an external force. However, using external forces not only involves the acceleration of atoms that may change the motional states of atoms, but also may be limited by the Bloch oscillation of atoms in optical lattices. Recently, a lot of attention has been focused on the quantum transport of atoms in optical lattices without involving external forces [21,22]. For instance, it has been proposed that quantum transport of atoms may be achieved in optical double-well lattices through the fast periodic modulation (in a nonadiabatic manner) of the inter- and intra-well tunnelings [21]. It was also proposed [22] that a fast oscillating linear potential in optical lattices can yield the quantum ratchet effect due to coherent destruction of tunneling [23], leading to quantum transport of atoms. However, all these schemes require accurate control of the lattice parameters and their time variation.

In this paper, we study the quantum transport of ultracold bosonic atoms in optical lattices without involving the accurate control of the lattice parameters and their time dependence. We consider atoms that are initially prepared in a certain region of a double-well optical lattice [24–34]. We show that a quantized number of atoms can be transferred to another region of the lattice through periodic and slow modulation of the optical lattice parameters (intra- and inter-well tunneling, chemical potential, etc.). Such quantized atom pumping may serve as a quantum atom battery for atomtronic devices. Note that there is an important difference between atom transport in optical lattices and charge transport in solids. While the electrons in solids are fermions, cold atoms in optical lattices can be bosons; therefore the Bose-Einstein statistics, instead of the Fermi-Dirac statistics, governs the transport dynamics. This important difference will be illustrated in this paper. Another important difference is that while electrons are periodically distributed in crystals, the density distribution of atoms can be prepared locally in the optical lattice and transferred to another region through the quantum transport process with periodic modulation of the lattice parameters. We emphasize that although periodic modulation of the lattice parameters in the parameter space is needed in the transport process, the rate of change of the parameters and the initial and final values of each parameter during its variation do not need to be accurately controlled. This is because the transport process depends on

*Author to whom correspondence should be addressed: cwzhang@wsu.edu

 ©2011 American Physical Society

the topology of the loop in the parameter space, instead of the exact parameter loop or the rate of change of the parameters along the loop. Therefore the quantum transport process is very robust against errors in the parameter modulation.

We find that the transport of bosonic atoms depends strongly on the atom filling per double well as well as the interaction. The strongly interacting bosonic atoms behave similarly to the noninteracting fermions with quantized transport at the half filling and no mass transport at the integer filling. In the weakly interacting region, the number of transported atoms is proportional to the atom filling. The investigation is based on the numerical simulation of the exact quantum dynamics of cold atoms in double-well optical lattices using the time evolving block decimation (TEBD) algorithm [35,36]. The transport properties observed in the numerical simulation are also understood by developing an analytical theory using a semiclassical transport model in the noninteracting and strongly interacting limits.

The paper is organized as follows. Section II describes the physical system: the cold bosonic atoms in a double-well optical lattice. Section III presents the numerical results on the transport of bosonic atoms in the optical lattices through periodic modulation of the lattice parameters. In Sec. IV, we provide a semiclassical transport model to explain the numerically observed transport of bosonic cold atoms in the noninteracting and strongly interacting limits. Section V consists of conclusions.

II. COLD BOSONS IN DOUBLE-WELL OPTICAL LATTICES

Consider ultracold bosonic atoms confined in a one-dimensional double-well optical lattice [Fig. 1(a)]. An optical lattice is a standing wave of coherent off-resonance light created by the interference of two or more laser beams. In experiments, the 1D double-well optical lattice has been realized by superimposing two laser beams with two different wavelengths $\lambda_2 = \lambda_1/2$ [24–27], or the Fourier synthesis of asymmetric optical potentials with spatial periodicity $\lambda/2n$ (n is an integer) [37]. In these experiments, the dynamics along the other two dimensions are frozen to the ground states by optical lattices with high potential depths ($\gg$ recoil energy). With the standard tight-binding approximation, the dynamics of atoms in the double-well optical lattices can be described by a Bose-Hubbard Hamiltonian [38],

$$H = -\sum_{j=1}^{N-1}\left[\frac{J}{2} - (-1)^j\frac{\delta}{2}\right](a_j^\dagger a_{j+1} + \text{c.c.}) + \sum_{j=1}^{N-1}[V_j + (-1)^{j+1}\Delta]n_j + Un_j(n_j-1), \quad (1)$$

where $[J-(-1)^j\delta]/2$ describes the inter- or intra-well tunneling, V_j is the external potential (e.g., the harmonic trap, disorder, etc.), 2Δ is the chemical potential difference between two neighboring lattice sites in a double well, and U is the on-site interaction strength between atoms. In experiments, the tunneling $[J-(-1)^j\delta]/2$ can be adjusted by varying the intensities of the two laser beams, the chemical potential Δ can be tuned by shifting one laser beam with respect to the other, the on-site interaction U between atoms can be changed using the Feshbach resonance [39], and the disorder potential can be created using optical speckle potentials [40].

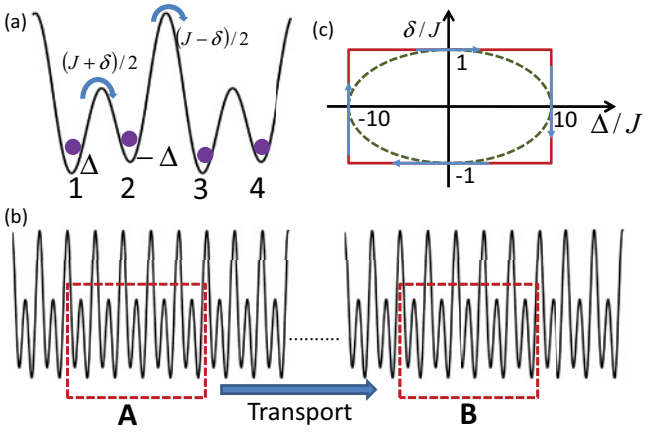

FIG. 1. (Color online) Schematic plot of the quantum transport of ultracold bosonic atoms in a double-well optical lattice. (a) Illustration of the double-well optical lattice parameters. (b) Illustration of the quantum transport process of bosonic atoms from region A to region B in the lattice. (c) The periodic modulation of the lattice parameters for the quantum transport process. Two different types of loops in the parameter space are considered: square (solid line) and elliptical (dashed line).

The transport process of cold atoms is illustrated in Fig. 1(b). Initially, the bosonic atoms are confined within a group of lattice sites (denoted as region A) using a harmonic or box trapping potential [41], which will be removed after the transport starts. The transport is realized by moving the atoms in the region A to another group of lattice sites (denoted as region B) by modulating the lattice parameters periodically, but without the actual movement of the lattice. Therefore it is a quantum transport process through the tunneling dynamics. To simplify the study, we assume a uniform distribution of the atoms in region A at time $t = 0$. During the transport process, the lattice parameters δ and Δ are tuned along a periodic closed loop in the parameter space, as illustrated in Fig. 1(c).

The time-dependent dynamics of atoms in the optical lattice are investigated numerically using the TEBD algorithm [35,36]. The TEBD algorithm is an effective method for simulating the exact one-dimensional quantum dynamics when the quantum entanglement of the system is low. It works well for the Hamiltonian (1) where the only nonlocal terms are the nearest neighboring tunneling. To check the validity of our numerical program, we have compared the results from the TEBD and that from the exact diagonalization for a small lattice system and they agree with a high accuracy. Henceforth, we set the energy unit of the system as J, and the time unit as J^{-1}.

We assume the initial parameter $\delta/J = 1$ to obtain a well-defined localized initial state. With this parameter, the inter-well tunneling vanishes and the initial wave function of the system is a product of the wave function in each double well. We use the number states of atoms at each lattice site as the basis states to represent the wave function. For instance, consider a double-well lattice with a lattice length $N = 20$ and $\Delta/J = 0$ initially. Ten atoms are uniformly distributed in the

region A between sites 5 and 14. In the region A, the wave function in the lth double well can be written as

$$\psi_l = c_{20}|20\rangle_l + c_{02}|02\rangle_l + c_{11}|11\rangle_l, \tag{2}$$

where

$$c_{20} = c_{02} = \sqrt{\frac{J^2}{(\sqrt{U^2+4J^2}+U)\sqrt{U^2+4J^2}}},$$

$$c_{11} = \sqrt{\frac{\sqrt{U^2+4J^2}+U}{2\sqrt{U^2+4J^2}}}.$$

$|nm\rangle$ is the state with n (m) atoms in the left (right) well. Outside region A, the wave function in each double well is simply $\phi_l = |00\rangle_l$.

The quantum transport process is accomplished by modulating the lattice parameters (δ,Δ) periodically in the parameter space, as illustrated in Fig. 1(c). Two different loops (square and elliptical) are considered and their effects will be discussed later in the paper. We choose the rate of the change of the parameters (δ,Δ) such that the tunneling process is adiabatic in each double well and the atoms always stay on the ground state of the double well. During the whole transport process, the atoms are assumed to be on the motional ground state at each lattice site. This assumption can be realized by using a double-well lattice with an intra-well potential depth $V_L \sim 6E_R$, where $E_R = \frac{h^2}{2m\lambda^2}$ is the atom recoil energy, h is the Planck constant, λ is the wavelength of the short-wavelength laser, and m is the atom mass. This potential depth yields a tunneling rate $J \sim 0.05E_R$ [42]. Therefore the required chemical potential shift $\Delta \sim 0.5E_R$ for the transport process is much smaller than the energy gap between the ground and first excited motional bands (typically several E_R).

In each isolated double well with two atoms, the Hamiltonian can be written as

$$H_d = \begin{pmatrix} 2\Delta+U & 0 & -J \\ 0 & -2\Delta+U & -J \\ -J & -J & 0 \end{pmatrix} \tag{3}$$

on the basis $\{|20\rangle,|02\rangle,|11\rangle\}$. Without interaction between atoms ($U=0$), the eigenenergies are $E_\pm = \pm\sqrt{4\Delta^2+2J^2}$, $E_3 = 0$. Therefore the energy gap between the ground state E_- and the first excited state E_3 is larger than $\sqrt{2}J$. In the presence of strong interaction U (neglect Δ), the three eigenenergies are $E_\pm = \frac{1}{2}U(1 \pm \sqrt{1+8J^2/U^2})$, $E_3 = U$. The energy gap between the ground state E_- and the first excited state E_3 is $\sim U$. The crossover between different energy bands in Fig. 2 is essentially a Landau-Zener tunneling process. In both parameter regions, the Landau-Zener adiabatic criteria in the double well can be easily satisfied by requiring $\frac{d\Delta}{dt} = 2\epsilon_1 J^2$ along the horizontal loop in Fig. 1(c). Along the vertical loop, we choose $\frac{d\delta}{dt} = \epsilon_2\Delta^2$ to avoid the tunneling between two wells with different chemical potentials. Here $\epsilon_1 = 0.1 \ll 1$, $\epsilon_2 = 0.01 \ll 1$ are the adiabatic parameters. The energy gap is also numerically calculated and plotted in Fig. 2 for general parameters. We see that the gap is always larger than $\sqrt{2}J$ for different Δ and U. When the lattice parameters are modulated along the elliptical loop in Fig. 1(c), there is no overall adiabaticity among double wells because atoms can now diffuse to a long distance if a long time period is used for the parameter modulation. Since the change of the parameters is slow, the cycle frequency of the periodic lattice modulation is much smaller than the energy gap.

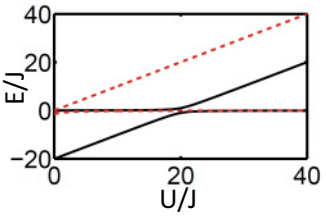

FIG. 2. (Color online) Plot of the lowest two eigenenergies with respect to U for two atoms in a double well. Solid line: $\Delta = 0$. Dashed line: $\Delta = 10J$.

In the case of one atom per double well, the Hamiltonian in each double well can be written as

$$H_s = \begin{pmatrix} \Delta & -J \\ -J & -\Delta \end{pmatrix} \tag{4}$$

on the basis $\{|10\rangle,|01\rangle\}$. The eigenenergies are $E_\pm = \pm\sqrt{\Delta^2+J^2}$ and the minimum energy gap is $2J$; therefore the above rate of change of the lattice parameters still keeps the adiabaticity in each double well.

III. QUANTUM TRANSPORT IN DOUBLE-WELL OPTICAL LATTICES

We numerically integrate the time-dependent Schrödinger equation with the Hamiltonian (1) using the TEBD algorithm and calculate the density distribution of atoms at different lattice sites. In Fig. 3, we plot the number of atoms at lattice sites 15 and 16 after one cycle of the parameter modulation described in Fig. 1(c). The lattice system contains total $N = 20$ sites with 10 atoms uniformly distributed between sites 5 and 14. Clearly the number of atoms transported to the neighboring double well (sites 15 and 16) depends on the interaction and the parameter modulation loop. In the weak interaction region ($U < \Delta$), two atoms are transferred to sites 15 and 16, which are the same as for noninteracting bosons. In the case of noninteracting bosons, atoms follow the changes of the potential minima in the lattice system and it is easy to see that atoms would like to move one double-well distance (two lattice sites) after one cycle of the parameter modulation. As the interaction increases, there is a sharp transition for the

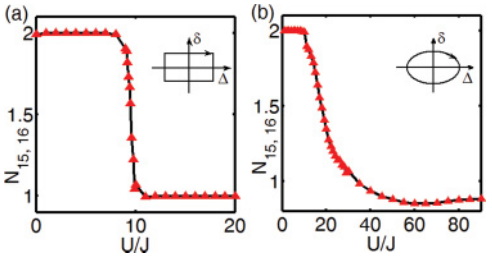

FIG. 3. (Color online) Plot of the number of atoms in the lattice sites 15 and 16 with respect to the atom interaction strength U after one cycle of the parameter modulation illustrated in the insets. Initially ten atoms uniformly occupy the lattice sites 5 to 14. (a) A square loop. (b) An elliptical loop.

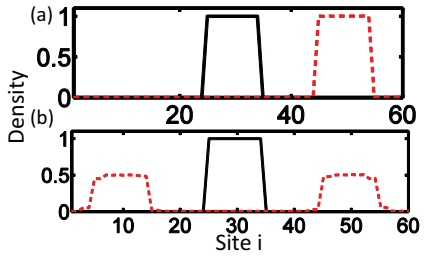

FIG. 4. (Color online) Plot of the density distribution of atoms after 10 cycles of the parameter modulation with the square loop. Solid line: Initial density distribution. Dashed line: Final density distribution. (a) $U = 5J$. (b) $U = 20J$.

square loop, where the number of the transported atoms at sites 15 and 16 becomes one [Fig. 3(a)]. In this region, the atoms behave the same as noninteracting fermions, and two atoms cannot occupy the same lattice site. The same physical picture applies to more cycles of the parameter modulation. In Fig. 4, we plot the density distribution of atoms after 10 cycles of the parameter modulation. For a small interaction strength, the atoms are transported to a target region that is 20 lattice sites away from the original region [Fig. 4(a)]. For a large interaction strength, atoms move to both left and right directions [Fig. 4(b)], and the center of mass of the atoms does not change (i.e., no mass transport).

When the parameter modulation is along the elliptical loop, there is a diffusion of the atoms along the lattices because the locally confined initial state is not the ground state of the Hamiltonian. In Fig. 3(b), we plot of the number of atoms at lattice sites 15 and 16 after one cycle of the parameter modulation along the elliptic loop. The main feature of Fig. 3(a) is still kept. In the weakly interacting region, the number of transported atoms is two, but the sharp transition is smoothed out and the number of atoms at the large U is no longer one because of the diffusion of the atoms through the lattice. In Fig. 5, we plot the density distribution of atoms after one cycle of the parameter modulation with a fixed $\Delta = 0$ and varying δ between 1 and -1. The diffusion of the atom density depends strongly on the rate of the change of the parameters. To suppress such uncontrolled diffusion, henceforth we mainly consider the square loop.

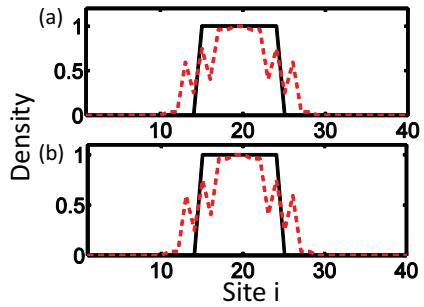

FIG. 5. (Color online) Plot of the diffusion of atoms after one cycle of the parameter modulation. Δ is fixed at 0. δ varies from J to $-J$ and then back to J. Solid line: Initial density distribution. Dashed line: Final density distribution after one cycle. (a) $U = 5J$. (b) $U = 20J$.

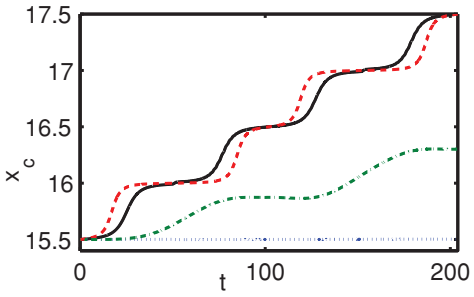

FIG. 6. (Color online) Plot of the center-of-mass motion of the atoms in one cycle of the potential modulation. Initially six atoms are uniformly distributed in three double wells. Solid line: $U = 5J$, square loop. Dashed line: $U = 5J$, elliptical loop. Dotted line: $U = 20J$, square loop. Dashed-dotted line: $U = 20J$, elliptical loop.

The atom transport in the optical lattice can also be described using the center-of-mass (c.m.) motion of the atoms. In Fig. 6, we plot the c.m. motion of atoms in the double-well lattice after one cycle of the parameter modulation. We see in the weakly interacting region that the c.m. is shifted by two lattice site for both elliptical and square loops. In the strongly interacting region, the c.m. does not change for the square loop, indicating no mass transport, but varies for the elliptical loop, showing the asymmetry of the diffusion process in the parameter modulation process.

In the above discussion, we assume that there are two atoms per double well (i.e., integer filling) in the initial state. Another interesting region is the half filling, that is, one atom per double well. In Fig. 7, we plot the c.m. motion of atoms after one cycle of the parameter modulation at the half filling. In both weakly and strongly interacting regions, the shift of the c.m. is two lattice sites, indicating that the noninteracting bosons and fermions behave similarly at the half filling although their transport properties are completely different at the integer filling. The elliptical and square loops also yield similar results.

In addition to the double-well optical lattice potential, the atoms may also experience an overall harmonic trapping potential. In Fig. 8, we plot the transport of atoms in the presence of a harmonic trap. Clearly the harmonic trapping potential does not affect the transport even far away from

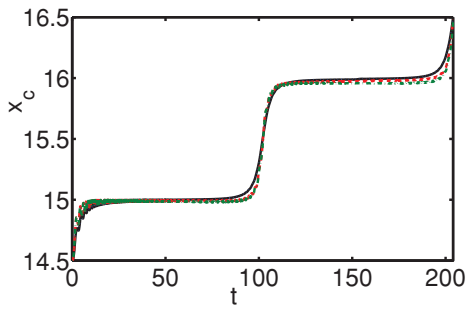

FIG. 7. (Color online) (a) Plot of the center-of-mass motion of the atoms in one cycle of the potential modulation. Initially six atoms are uniformly distributed in six double wells. Solid line: $U = 5J$, square loop. Dashed line: $U = 5J$, elliptical loop. Dotted line: $U = 20J$, square loop. Dashed-dotted line: $U = 20J$, elliptical loop.

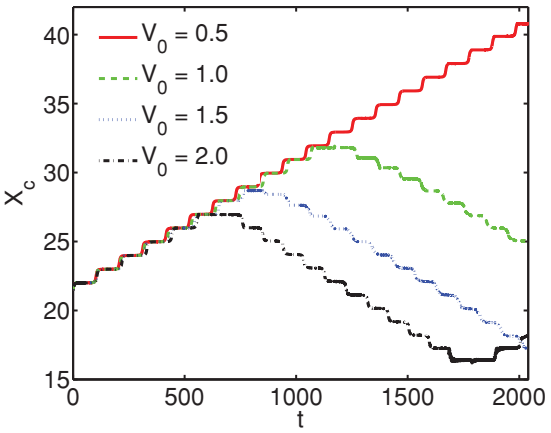

FIG. 8. (Color online) The transport of atoms in the presence of a harmonic trapping potential $V_i = V_0(i - x_o)^2$, where x_o locates at the center of the lattice.

the trap center. More interestingly, the initial right-moving c.m. motion turns to the left-moving motion after it reaches the maximum position that is determined by the harmonic trapping frequency. In a realistic experiment, this phenomenon corresponds to a dipole oscillation of atoms generated by the periodic modulation of the lattice parameters. The turnaround can be understood from the fact that when the c.m. reaches certain x, the chemical potential difference 2Δ cannot overcome the potential difference between two wells induced by the harmonic trap. Therefore atoms do not move at that cycle. Further modulation of the lattice parameters then provides a driving of atoms to the left-moving direction.

Finally, we discuss how to observe the quantized atom transport in the double-well optical lattices. In principle, the transport dynamics can be observed using the single-atom detection technology demonstrated recently [43–46]. Here we consider the signature of quantum transport in more conventional experimental techniques: the momentum distribution in the time-of-flight image. The momentum distribution of the atoms in the optical lattices can be calculated as

$$n_{k,t} = \sum_{i,j} \langle \psi(t)|a_i^\dagger a_j|\psi(t)\rangle e^{ik(i-j)}. \tag{5}$$

The numerical results are shown in Fig. 9 for $U = 5J$ (a) and $U = 20J$ (b). In the weak-interacting case, the atoms in one double well are perfectly transported to another double well and the final density distribution simply has a global shift of the position; there we expect $n_{k,t} = n_{k,t+T}$ after one period, as shown in Fig. 9(a). In the strong-interacting case, the cold atoms move along two opposite directions; therefore $n_{k,t} \neq n_{k,t+T}$ and the coherent peaks in the momentum distribution disappear. We find the momentum distribution is generally independent of the loops used in TEBD calculations. In experiments, the momentum distribution can be measured directly from the time-of-flight image, thus providing a direct experimental signature for the quantum transport.

IV. A SEMICLASSICAL THEORY

Physically, the numerical results obtained in the above section at the half filling may be understood through the change

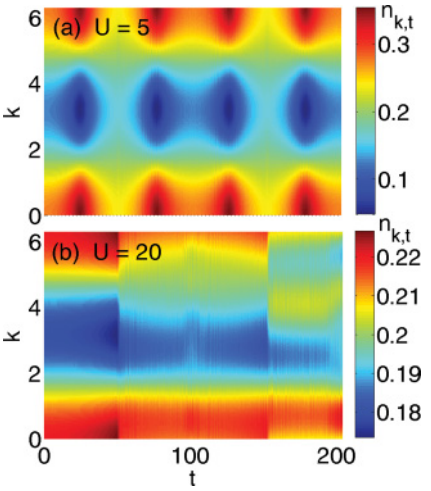

FIG. 9. (Color online) Plot of the momentum distribution of atoms in the time-of-flight image. (a) $U = 5J$. (b) $U = 20J$.

of the Wannier function of bosons in a periodic lattice due to the modulation of the lattice parameters. The center of the Wannier function follows the potential minimum of the double well, and can move from one double well to the neighboring one in one cycle. In this section, we present a semiclassical theory for the quantum transport of the noninteracting bosons in the double-well lattice to understand the numerical results observed in the above section. On the other hand, the strongly interacting bosonic atoms are equivalent to noninteracting fermionic atoms; therefore their transport properties are the same as those of the noninteracting electrons. For simplicity, we consider a periodic system to avoid the diffusion.

With a periodic boundary condition, we can transform the Hamiltonian (1) without the interaction ($U = 0$) to the quasimomentum space

$$H = \Gamma(q) \cdot \sigma \tag{6}$$

by using the Fourier transformation $a_{2j-1} = \sum_q e^{iq(2j-1)a/2} a_{q\uparrow}$, $a_{2j} = \sum_q e^{iqja} a_{q\downarrow}$, where $\Gamma(q) = (-J\cos\frac{qa}{2}, \delta \sin\frac{qa}{2}, \Delta)$, and the spin-up and spin-down correspond to the left and right sites of the double well. The Hamiltonian (6) has two energy bands $\alpha = \pm$ with the dispersion

$$\varepsilon_\alpha = \pm\sqrt{J^2\cos^2\frac{qa}{2} + \delta^2\sin^2\frac{qa}{2} + \Delta^2}. \tag{7}$$

The velocity of an atom in the bands satisfies the semiclassical equation of motion [47]

$$\dot{x}_\alpha(q,t) = \frac{\partial \varepsilon_\alpha}{\partial q} - \Omega^\alpha_{qt}, \tag{8}$$

where $\Omega^\alpha_{qt} = -2\mathrm{Im}\langle \frac{\partial \Phi_\alpha}{\partial q} | \frac{\partial \Phi_\alpha}{\partial t}\rangle$ is the αth-band Berry curvature in the momentum and time spaces;

$$\Phi_\alpha = \frac{1}{\sqrt{2\varepsilon_\alpha(\varepsilon_\alpha - \Delta)}} \begin{pmatrix} -\left(J\cos\frac{qa}{2} + i\delta\sin\frac{qa}{2}\right) \\ \varepsilon_\alpha - \Delta \end{pmatrix} \tag{9}$$

is the eigen-wave-function. The total particle transport along a close loop in the parameter space can be written as

$$c_T = \oint j(t)dt = \frac{1}{2\pi}\sum_{\alpha=\pm}\oint dt\int_{-\pi/a}^{\pi/a} f(\varepsilon_\alpha-\mu)\dot{x}_\alpha(q,t)dq, \tag{10}$$

where $j(t)$ is the atom number current and $f(\varepsilon_\alpha-\mu)$ is the Fermi-Dirac distribution $f(\varepsilon_\alpha-\mu)=1/\{\exp[(\varepsilon_\alpha-\mu)/k_BT]+1\}$ for fermionic atoms and the Bose-Einstein distribution $f(\varepsilon_\alpha)=1/\{\exp[(\varepsilon_\alpha-\mu)/k_BT]-1\}$ for bosonic atoms. For the noninteracting bosonic atoms, all atoms occupy the lowest energy state, the chemical potential μ loses its meaning, and total atom transport at zero temperature becomes

$$c_T = \frac{\eta}{a}\oint dt\dot{x}_-(q_{\min},t), \tag{11}$$

where only the lowest energy band has a contribution, $q_{\min}$ is the quasimomentum at the energy minimum, and η is the number of atoms in each double well. The energy minimum of the lowest band ε_- locates at $q_{\min}=0$ except for the parameter $\delta=\pm1$, where the band is flat and does not depend on q. Note that $\delta=\pm1$ corresponds to isolated double wells in the lattice (i.e., no inter-well tunneling); therefore the initial state of the system can be chosen with $q=0$.

In the case of noninteracting bosonic atoms with an initial $q=0$, the first term in $\dot{x}_-$ is $\frac{\partial\varepsilon_-}{\partial q}|_{q=0}=0$ and the second term is

$$\Omega_{0t}^- = \frac{a\delta J}{4}\frac{\partial}{\partial t}\frac{1}{(J^2+\Delta^2-\Delta\sqrt{J^2+\Delta^2})}. \tag{12}$$

Therefore the total atom transport along the square loop in Fig. 1(c) is

$$c_T = -\frac{\eta}{a}\oint dt\Omega_{0t}^- = \eta \tag{13}$$

when $\Delta\gg J$. When there are η atoms in each double well, there are η atoms pumped out the system, agreeing with the numerical results presented in Figs. 6 and 7 .

In the case of strongly interacting bosons, which is equivalent to noninteracting fermions, the atoms gradually occupy different q states as the number of filling increases. In the case of the half filling, the lowest energy band ε_- is fully occupied and the chemical potential μ lies at the gap between two bands. The total transported atoms can be shown to be $c_T=1$ using Eq. (10) [5], which agrees with the numerical results obtained in Fig. 7. In the case of the integer filling (two atoms per double well), both bands are fully occupied and $c_T=0$ because the Berry curvatures $\Omega_{qt}^+=-\Omega_{qt}^-$ for two bands and their contributions to c_T cancel with each other. This result agrees with the numerical results presented in Fig. 6.

Finally, we comment on the validity of using the periodic boundary condition in the semiclassical theory for the explanation of the numerical results observed in Sec. III. Equations (6), (7), and (11) are introduced by assuming a periodic boundary condition for a single atom and the fact that the atom occupies the Bloch eigenstate. In general, the periodic system is not equivalent to our system where the atoms are initially localized. However, because the initial state we choose is the product of the state in each isolated double well (no inter-well tunneling), and the atoms at different double wells do not affect each other (no interaction), the periodic system can be taken as multiple copies of our local system. Therefore the effect of the quantum transport and the essential physics should be the same for the periodic system and our local system, which justifies the agreement between the semiclassical theory and the numerical results. The difference between these two systems is that, in a periodic system, the change of the local atom density after a period cannot be observed because it is periodic. Instead, what can be observed is the current, whose integration in one period gives the number of transported atoms. In our local system, the transport of atoms is directly reflected in the density variation because the neighboring lattice sites are not occupied initially.

V. CONCLUSION

In conclusion, in this paper we study the quantum transport of ultracold bosonic atoms in double-well optical lattices where the lattice parameters can be periodically modulated. The transport of atoms depends strongly on the atom filling and the interaction. In the strongly interacting region, the bosonic atoms behave similarly as fermions with quantized transport at the half filling and no transport at the integer filling. In the weakly interacting region, the quantized transport is robust and the number of the pumped atoms is proportional to the atom filling per double well. A signature of the quantum transport of atoms in the momentum distribution is obtained. In addition to the numerical simulation of the transport dynamics of atoms in the double-well optical lattice using the TEBD algorithm, we develop a semiclassical model to explain the numerical results in the noninteracting and strongly interacting limits. Our scheme for the quantized atom transport does not involve accurate control of the lattice parameters and their time dependence, and thus may provide a robust way for distributing atoms in optical lattices, which is critically important for quantum computation in optical lattices as well as atomtronics applications.

ACKNOWLEDGMENTS

This work is supported by ARO (W911NF-09-1-0248) and DARPA-YFA (N66001-10-1-4025).

[1] D. J. Thouless, Phys. Rev. B **27**, 6083 (1983).
[2] Q. Niu, Phys. Rev. Lett. **64**, 1812 (1990).
[3] M. Switkes, C. M. Marcus, K. Campman, and A. C. Gossard, Science **283**, 1905 (1999).
[4] L. Altshuler and L. I. Glazman, Science **283**, 1864 (1999).
[5] D. Xiao, M.-C. Chang, and Q. Niu, Rev. Mod. Phys. **82**, 1959 (2010).
[6] M. V. Berry, Proc. R. Soc. London A **392**, 45 (1984).

[7] M. D. Blumenthal, B. Kaestner, L. Li, S. Giblin, T. J. B. M. Janssen, M. Pepper, D. Anderson, G. Jones, and D. A. Ritchie, Nature Phys. **3**, 343 (2007).
[8] M. W. Keller, A. L. Eichenberger, J. M. Martinis, and N. M. Zimmerman, Science **285**, 1706 (1999).
[9] R. D. King-Smith and D. Vanderbilt, Phys. Rev. B **47**, 1651 (1993).
[10] G. Ortiz and R. M. Martin, Phys. Rev. B **49**, 14202 (1994).
[11] R. Resta, Rev. Mod. Phys. **66**, 899 (1994).
[12] I. Zutic, J. Fabian, and S. Das Sarma, Rev. Mod. Phys. **76**, 323 (2004).
[13] P. Sharma, Science **307**, 531 (2005).
[14] D. D. Awschalom and M. E. Flatté, Nature Phys. **3**, 153 (2007).
[15] B. T. Seaman, M. Krämer, D. Z. Anderson, and M. J. Holland, Phys. Rev. A **75**, 023615 (2007).
[16] R. A. Pepino, J. Cooper, D. Z. Anderson, and M. J. Holland, Phys. Rev. Lett. **103**, 140405 (2009).
[17] M. G. Raizen, A. M. Dudarev, Q. Niu, and N. J. Fisch, Phys. Rev. Lett. **94**, 053003 (2005).
[18] A. Cho, Science **320**, 312 (2008).
[19] I. Bloch, J. Dalibard, and W. Zwerger, Rev. Mod. Phys. **80**, 885 (2008).
[20] M. Lewenstein, A. Sanpera, V. Ahufinger, B. Damski, A. Sen De, and U. Sen, Adv. Phys. **56**, 243 (2007).
[21] O. Romero Isart and J. J. García-Ripoll, Phys. Rev. A **76**, 052304 (2007).
[22] C. E. Creffield, Phys. Rev. Lett. **99**, 110501 (2007).
[23] F. Grossmann, T. Dittrich, P. Jung, and P. Hänggi, Phys. Rev. Lett. **67**, 516 (1991).
[24] J. Sebby-Strabley, M. Anderlini, P. S. Jessen, and J. V. Porto, Phys. Rev. A **73**, 033605 (2006).
[25] J. Sebby-Strabley, B. L. Brown, M. Anderlini, P. J. Lee, W. D. Phillips, J. V. Porto, and P. R. Johnson, Phys. Rev. Lett. **98**, 200405 (2007).
[26] S. Trotzky, P. Cheinet, S. Fölling, M. Feld, U. Schnorrberger, A. M. Rey, A. Polkovnikov, E. A. Demler, M. D. Lukin, and I. Bloch, Science **319**, 295 (2008).
[27] G. De Chiara, T. Calarco, M. Anderlini, S. Montangero, P. J. Lee, B. L. Brown, W. D. Phillips, and J. V. Porto, Phys. Rev. A **77**, 052333 (2008).
[28] P. Barmettler, A. M. Rey, E. Demler, M. D. Lukin, I. Bloch, and V. Gritsev, Phys. Rev. A **78**, 012330 (2008).
[29] A. M. Rey, V. Gritsev, I. Bloch, E. Demler, and M. D. Lukin, Phys. Rev. Lett. **99**, 140601 (2007).
[30] M. R. Peterson, C. Zhang, S. Tewari, and S. Das Sarma, Phys. Rev. Lett. **101**, 150406 (2008).
[31] I. Danshita, J. E. Williams, C. A. R. Sá de Melo, and C. W. Clark, Phys. Rev. A **76**, 043606 (2007).
[32] S. Trebst, U. Schollwöck, M. Troyer, and P. Zoller, Phys. Rev. Lett. **96**, 250402 (2006).
[33] V. G. Rousseau, D. P. Arovas, M. Rigol, F. Hébert, G. G. Batrouni, and R. T. Scalettar, Phys. Rev. B **73**, 174516 (2006).
[34] P. Schlagheck, F. Malet, J. C. Cremon, and S. M. Reimann, New J. Phys. **12**, 065020 (2010).
[35] G. Vidal, Phys. Rev. Lett. **93**, 040502 (2004).
[36] See [http://physics.mines.edu/downloads/software/tebd/] for a detailed note on the TEBD algorithm.
[37] G. Ritt, C. Geckeler, T. Salger, G. Cennini, and M. Weitz, Phys. Rev. A **74**, 063622 (2006).
[38] D. Jaksch, C. Bruder, J. I. Cirac, C. W. Gardiner, and P. Zoller, Phys. Rev. Lett. **81**, 3108 (1998).
[39] C. Chin, R. Grimm, P. Julienne, and E. Tiesinga, Rev. Mod. Phys. **82**, 1225 (2010).
[40] L. Sanchez-Palencia and M. Lewenstein, Nature Phys. **6**, 87 (2010).
[41] U. Schneider *et al.*, e-print arXiv:1005.3545.
[42] M. Greiner, Ph.D. thesis, Ludwig Maximilians Universitaet Muenchen, Germany, 2003.
[43] W. S. Bakr, J. I. Gillen, A. Peng, S. Fölling, and M. Greiner, Nature (London) **462**, 74 (2009).
[44] J. F. Sherson, C. Weitenberg, M. Endres, M. Cheneau, I. Bloch, and S. Kuhr, Nature (London) **467**, 68 (2010).
[45] C. Weitenberg, M. Endres, J. F. Sherson, M. Cheneau, P. Schauß, T. Fukuhara, I. Bloch, and S. Kuhr, Nature (London) **471**, 319 (2011).
[46] C. Zhang, S. L. Rolston, and S. Das Sarma, Phys. Rev. A **74**, 042316 (2006).
[47] G. Sundaram and Q. Niu, Phys. Rev. B **59**, 14915 (1999).